Current Journal of Applied Science and Technology

37(5): 1-15, 2019; Article no.CJAST.51593

ISSN: 2457-1024
(Past name: British Journal of Applied Science & Technology, Past ISSN: 2231-0843, NLM ID: 101664541)

Study of the Output Electric Parameters of the Sub-cells Composing the $Ga_{0.67}In_{0.33}P/GaAs/Ga_{0.70}In_{0.30}As$ Triple-Junction Photovoltaic Cell and its Performance in Real Environment:Cases of Bujumbura and Bugarama in Burundi

N. Ndorere[1,2*], B. Kounouhewa[2] and M. B. Agbomahena[3]

[1] *Institut de Mathématiques et de Sciences Physiques (IMSP), Université d'Abomey-Calavi (UAC) 01BP 526 Cotonou, Benin.*

[2] *Laboratoire de Physique du Rayonnement (LPR), Université d'Abomey-Calavi (UAC) 01BP 526 Cotonou, Benin.*

[3] *Laboratoire de Caractérisation Thermophysique des Matériaux et Appropriation Energétique (Labo CTMA), Université d'Abomey-Calavi (UAC) 01BP 526 Cotonou, Benin.*

Authors' contributions

This work was carried out in collaboration with all the authors. Author N. Ndorere designed the study, developed the analytical prediction model, performed simulations using Matlab software and wrote the first version of the manuscript. Prof. B. Kounouhewa and Dr. M. B. Agbomahena have made significant contributions as supervisors, particularly in data processing and results analysis. All authors have read and approved the final manuscript.

Article Information

DOI: 10.9734/CJAST/2019/v37i530304
Editor(s):
(1) Dr. Rodolfo Dufo López, Electrical Engineer, Ph. D. Electrical Engineering Department, University of Zaragoza, Calle María de Luna, 3 (Edificio Torres Quevedo) 50018 Zaragoza, Spain.
(2) Dr. Koji Nagata, Department of Physics, Korea Advanced Institute of Science and Technology, Daejeon, Korea.
Reviewers:
(1) Aleksandra Vasic-Milovanovic, University of Belgrade, Serbia.
(2) Wen bo xiao, Nanchang Hangkong University, China.
Complete Peer review History: http://www.sdiarticle4.com/review-history/51593

Received: 14 July 2019
Accepted: 21 September 2019
Published: 26 September 2019

Original Research Article

ABSTRACT

Multi-junction photovoltaic cells composed of III-V semiconductor materials are widely used in photovoltaic systems. They offer very high efficiencies compared to single-junction photovoltaic cells. Knowledge of the behavior of their electrical parameters in real operating conditions is essential for their best use. This work presents an analytical model for predicting the behavior of the output electrical parameters of the sub-cells composing the $Ga_{0.67}In_{0.33}P/GaAs/Ga_{0.70}In_{0.30}As$

**Corresponding E-mail: ndoreregity@gmail.com;*

triple junction photovoltaic cell, operating under the actual conditions of two selected sites. The dependence of the external quantum efficiency at the wavelengths corresponding to the absorption ranges of the top $(Ga_{0.67}In_{0.33}P)$, middle $(GaAs)$ and bottom $(Ga_{0.70}In_{0.30}As)$ sub-cells is analyzed and discussed. The influence of temperature and irradiation on the Voc, Jsc, FF and η parameters is discussed taking into account the meteorological characteristics of two selected locations. An average daily conversion efficiency of the Triple-Junction solar cell of 37.24% and a daily electrical power of $1613.1W/m^2$ for the typical day(TD) of the sunniest month of the Bujumbura site were found. Similarly, under the same conditions, for the Bugarama site, we found an average daily efficiency of 37.28% and a daily electrical power of $1619.7W/m^2$. The developed model can also be used to design a more suitable Photovoltaic system at any specified place, provided that local weather data is available.

Keywords: Triple-junction solar cell; III-V semiconductor; Weather conditions; model.

1 INTRODUCTION

Tropical zone countries face growth challenges due to insufficient energy supply. Burundi, one of these countries, has been experiencing a chronic energy crisis for years despite significant hydropower, solar and wind power potential. It has various energy resources including water resources, wind, solar and biomass but they are weakly or not at all exploited. The exploitable hydroelectric potential is approximately $1300MW$, but only $32MW$ are exploited. Access to electrical energy is very deplorable. Only 5% of the population has access to electricity among them, most live in Bujumbura the economic capital of the country, the average annual consumption of electricity per inhabitant is $23kWh/year$ [1-2]. Faced with this deficit, small autonomous solar PV systems become an attractive and promising alternative, for independent household power supply or social amenities such as schools, health centers, hospitals, pumping stations and some local administrative offices in the off-grid area. For several years, the rate of production and use of photovoltaic energy has steadily increased. This has led to various researches on the various aspects of the PV system, the development of new cells, performance analysis, sizing and optimization of the structure of photovoltaic systems [3-4].

Currently, multi-junction photovoltaic cells composed of $III-V$ semiconductor materials are widely used in photovoltaic systems. They offer very high efficiency compared to mono-junction photovoltaic cells such as those made of silicon, which are largely used in the world. The characterization of photovoltaic cells is generally done in the laboratory under standard conditions that is to say, the temperature of $25\deg C$ or $28\deg C$ and irradiance of $1000W/m^2$ or $1367W/m^2$, if they are intended to terrestrial or space applications. However, in many applications, the actual operating conditions differ greatly from these laboratory conditions. Thus, knowledge of the behavior of the electrical parameters of multi-junction photovoltaic cells is essential for terrestrial and space applications.

Studies on the influence of temperature and irradiance on the output parameters of Multi-junction photovoltaic cells have been analyzed in detail in several references, including refs[5-6]. Experimental work on the temperature dependence of the external quantum efficiency (EQE) of a Multi-junction solar system composed of III-V semiconductor materials have been reported in several references including the refs[7-8]. In addition, the existing literature covers several experimental studies that have focused mainly on the influence of temperature and irradiance on the performance of multi-junction PV solar cells without thorough investigation of the behavior of their respective sub-cells. Thus, predicting the energy production of photovoltaic systems using tri-junction solar cells remains a challenge [9]. The efficiencies of such systems are strongly influenced by the environmental and climatic conditions of the installation site.

The tri-junction PV solar cell that is the subject of our study consists of three serially interconnected sub-cells composed of $Ga_{0.67}In_{0.33}P$ (top sub-cell), $GaAs$ (middle sub-cell) and $Ga_{0.70}In_{0.30}As$

(bottom sub-cell).These sub-cells are placed, from top to bottom, in a decreasing order of their gap energies, which allows efficient use of the solar spectrum. Through serial interconnection, knowledge of sub-cell parameter behavior allows assertions on the associated tri-junction solar cell.

In this work, we will develop a simple model that predicts, firstly, the behavior of the output parameters (Voc, Jsc, FF and η) of the sub-cells composing the $Ga_{0.67}In_{0.33}P/GaAs/Ga_{0.70}In_{0.30}As$ triple junction photovoltaic cell, then the variability of the external quantum efficiency (EQE) of the latter as a function of the wavelengths corresponding to their absorption ranges and finally the performance of this cell in the actual meteorological conditions of the sites considered.The choice of the gallium and indium molar composition of the semiconductor materials of the top and bottom sub-cells has been guided by the desired gap energies.

2 MATERIALS AND METHODS

2.1 Location of Studied Sites

Burundi is a country located in East Africa and partly in Central Africa.It is surrounded by three countries: Tanzania in the East, Rwanda in the North, the Democratic Republic of Congo in the West and is bordered by Lake Tanganyika in the South-west. The geographical position of Burundi normally gives it an equatorial and tropical climate characterized by abundant rainfall for several months of the year and low thermal amplitudes [10]. Local complications are observed under the influence of the relief characterized by the presence of plains, plateaus, mountain ranges and depressions of the North-East. These physical factors influence the distribution of climatic parameters, in this case precipitation and air temperatures. Altitude is the main factor of variation of temperature in Burundi.

The spatial distribution of the temperature closely marries the great orographic units of the country. The first selected site that of Bujumbura, is located in the natural region of Imbo with an altitude of less than 1000 m and an average temperature between $23\deg C$ and $24.5\deg C$. This site is located west of the country along Lake Tanganyika in an area of lowland plains (774-1000 m) with a warm tropical climate $(23\deg C)$ average temperature), low rainfall (800-1000 mm / year) and a dry season of five to six months. The second site, Bugarama, is located in the Mugamba natural region, on the Congo-Nile ridge where the altitude ranges from 2000 to 2670 m. The area is characterized by annual rainfall between 1500 and 2000 mm, and an equatorial mountain climate with average annual temperatures of $12\deg$ to $16\deg C$ [10]. The irradiation and temperature data used in the Bujumbura sites (latitude$322'55"$and longitude $29\deg 21'51"$) and Bugarama (latitude is $2\deg 53'5"$South and longitude $29\deg 34'14"$East") were found using MERRA (Modern-Era Retrospective Analysis for Re-search and Applications).

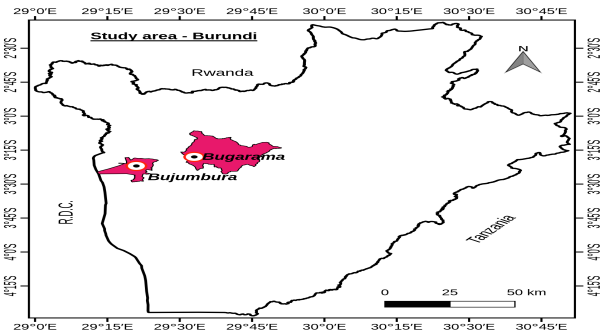

Fig. 1. Geographical location of Burundi, the roundabouts represent the studied sites namely Bujumbura and Bugarama.

2.2 Properties of the Semiconductor Materials Constituting the $Ga_{0.67}In_{0.33}P/GaAs/Ga_{0.70}In_{0.30}As$ Solar Cell.

$Ga_xIn_{1-x}P$ is a ternary material composed of G_aP and I_nP two binary materials. It has a direct gap for a gallium mole fraction less than 0.77 and an indirect gap if not [11]. It has no defect related to incorporation with oxygen during its growth and has a low rate of recombination at the surface. The properties of $Ga_xIn_{1-x}P$ material are shown in Table 1;

Table1. Optoelectronic properties of $Ga_xIn_{1-x}P$ at $300K$

Parameters	$Ga_xIn_{1-x}P$	$Ga_{0.67}In_{0.33}P$	Ref
Gap energy Eg(x)	$0.65x^2$+0.27x+1.34	1.93	[12]
density(gcm^{-3})	4.81-0.67x	4.2941	[13]
coef of thermal expansion $\alpha(\times 10^{-6}C^{-1})$		5.3	[3]
static electric constant ε_s	$\varepsilon_s = 12.5 - 1.4x$	11.4220	[13]
electronic affinity χ	$\chi(x) = 4.38 - 0.58x$	3.93	[13]
Auger coefficient $A(cm^6/s)$	$A(x) = -8.210^{-30}x^2$		
	$+8.310^{-30}x + 910^{-31}$	2.4292×10^{-30}	[12]
radiactive recombination $A_0(cm^3/s)$	$A_0(Eg) = -2.36210^{-10}Eg^2$		
	$+7.20210^{-10}Eg - 4.21410^{-10}$	8.876510^{-11}	[12]
density effective states Nc	$Nc = 2(\pi qkTm_e^\star/h^2)^{3/2}$	6.5×10^{17}	[12-14]
density effective states Nv	$Nv = 2(\pi qkTm_h^\star/h^2)^{3/2}$	1.45×10^{19}	[13-14]
effective mass of electrons	$\frac{m_e^\star}{m_0} = 0.0254x^2 - 0.114x + 0.08$	15×10^{-3}	[12-15]
effective mass of holes	$\frac{m_h^\star}{m_0} = 0.19x + 0.6$	72.73×10^{-2}	[15]
concentration carriers intrinsic n_i	$n_i = \sqrt{N_cN_vexp[-Eg/2kT]}$	$2.3861e+10$	[13-15]

The $GaAs$ is a material with a direct gap. In comparison than with silicon, it has a high absorption coefficient (90% of the photons are absorbed in a thickness of $3\mu m$), it has a high mobility of minority carriers, a high resistance to solar radiation and a high stability to high temperature [16]. GaAs is known as the most suitable material for photovoltaic conversion, thanks to its direct band gap of $1.42eV$, which adapts well with the solar spectrum.

Table 2. The electronic and crystalline properties of $GaAs$ at $300K$

Parameters	$GaAs$	Ref
Gap energy Eg(x)	1.42	[15]
density(gcm^-3)	5.360	
	5.32	[15-16]
coefficient of thermal expansion $\alpha(\times10^-6C^-1)$	5.76	[16]
dielectric constant ε_r	13.18	
	12.9	[15]
electronic affinity χ	4.07	[15]
Auger coefficient $A(cm^6/s)$	Dope(n) : 1.9×10^{-31}	
	Dope(p) : 12×10^{-31}	[16]
radiactive recombination $A_0(cm^3/s)$	10^{-10}	[16]
density effective states Nc	4.7×10^{17}	[12,13,16]
density effective states Nv	9.8×10^{18}	[12,13,16]
effective mass of electrons	$\frac{m_e^\star}{m_0} = 0.0670$	[16-19]
effective mass of holes	$\frac{m_h^\star}{m_0} = 0.642$	[13,14,15,17]
concentration carriers intrinsic n_i	$n_i = \sqrt{NcNv}exp[-Eg/2kT] = 2.1 \times 10^6$	[12,13,16]

$Ga_xIn_{1-x}As$ is a ternary material composed of GaAs and InAs two binary materials.It is a semiconductor material that is promising in the photovoltaic field because it has a direct gap across its composition range and a high absorption coefficient in the long wavelength domain (domain of the infrared).

Table 3. The optoelectronic properties of $Ga_xIn_{1-x}AS$ at $300K$

Parameters	$Ga_xIn_{1-x}AS$	$Ga_{0.7}In_{0.3}As$	Ref
Gap energy Eg(x)	$0.477x^2$-1.537x+1.42	1.00	[6]
density(gcm^-3)	4.81-0.67x	4.6090	[7]
static electric constant ε_s	$\varepsilon_s = 12.5 - 1.4x$	12.0800	[7]
electronic affinity χ	$\chi(x) = 4.38 - 0.58x$	4.2060	[7]
Auger coefficient $A(cm^6/s)$	$A(x) = -8.210^{-30}x^2$ $+8.310^{-30}x + 910^{-31}$	2.6520e-30	[8]
radiactive recombination $A_0(cm^3/s)$	$A_0(Eg) = -2.36210^{-10}Eg^2$ $+7.20210^{-10}Eg - 4.21410^{-10}$	6.2600e-11	[8]
density effective states Nc	$Nc = 2(\pi qkTm_e^\star/h^2)^{3/2}$	4.7664e+18	[7-9]
density effective states Nv	$Nv = 2(\pi qkTm_h^\star/h^2)^{3/2}$	2.4072e+20	[7-9]
effective mass of electrons	$\frac{m_e^\star}{m_0} = 0.0254x^2 - 0.114x + 0.08$	0.0481	[8-10]
effective mass of holes	$\frac{m_h^\star}{m_0} = 0.19x + 0.6$	0.6570	[8]
concentration carriers intrinsic n_i	$n_i = \sqrt{NcNv}exp[-Eg/2kT]$	3.3859e+19	[7-9-10]

The $Ga_{0.67}In_{0.33}P/GaAs/Ga_{0.70}In_{0.30}As$ solar cell is composed of three sub-cells which are arranged in series in descending order of their gap energies, where each sub-cell exploits the part of the solar spectrum adapted to its gap. They are interconnected electrically and optically by tunnel junctions. The performance of the tandem solar cell depends on the properties of the three sub-cells composing the structure (top, middle and bottom). All sub-cells are traversed by the same current, so they must check the current matching. The total voltage delivered by the cell will be the sum of all the voltages delivered by the sub-cells.

2.3 Analytical Model

The simple model is proposed to study the behavior of the sub-cell output parameters and the performance of the $Ga_{0.67}In_{0.33}P/GaAs/Ga_{0.70}In_{0.30}As$ tri-junction solar cell in the meteorological conditions of the study site. This behavior depends essentially on our case of two factors namely the average daily global radiation of the study area and the average daily temperature. The gap energies of the semiconductor materials of the sub-cells of the tri-junction solar cell have temperature dependence according to relation (1) [18].

$$E_g(T_c) = E_{g,Tref} - 0.0002677 \times (E_{g,Tref})\,(T_c - T_{ref}) \tag{2.1}$$

With T_c: the temperature of the cell and $Tref$: the reference temperature which is $300K$ for our case. T_c depends on the ambient temperature and the irradiance of the region considered. Equation (2) gives us the expression of the temperature of the cell [19]:

$$T_c = 1.14(T_a - T_{STC}) + 0.0175(G - 300) + 30 \tag{2.2}$$

where T_a is the ambient temperature, T_{STC} is the temperature under the standard conditions of the test, G is the irradiance. An important parameter must be introduced in this work; it is an External Quantum Efficiency (EQE), which gives the probability that an incident photon of energy $E = h\nu$ will give an electron to an external circuit [20]. It is given by relations (3, 4):

$$EQE(\lambda) = \frac{J_{sc}(\lambda)}{q\Phi(\lambda)} = \frac{hcJ_{sc}(\lambda)}{qP_{in}(\lambda)} \tag{2.3}$$

$$EQE(\lambda) = 1240\frac{J_{sc}(\lambda)[A/cm^2]}{\lambda[nm]P_{in}[wcm^{-1}]} \tag{2.4}$$

where $\Phi(\lambda$ is the flux of incident photons, h is the Planck constant and c is the speed of light in vacuum and J_{sc} is the short-circuit current density which is given under the ideal conditions ($R_s = 0$, $R_{sh} = \infty$ and $EQE = 100\%$).

$$J_{sc} = \int_{\lambda_i}^{\lambda_f} q\Phi(\lambda)\,\mathrm{d}\lambda \tag{2.5}$$

Under actual operating conditions, the short-circuit current density is a function of the temperature of the cell (T_c) and the irradiance of the study area (G).

$$J_{sc} = \frac{G}{G_{STC}}\left[J_{sc} + \mu_{J_{sc}}\left(T_c - T_{STC}\right)\right] \tag{2.6}$$

G_{STC} is the irradiance under standard test conditions $(1000W/m^2)$ and T_{STC} is the temperature under these same conditions $(25C)$ and $\mu_{J_{sc}}$ is the short-circuit current temperature coefficient.

The open-circuit voltage $(V_{oc}$, which represents a maximum voltage across the solar cell, for $(J_{sc} = 0)$, is given by [21]:

$$V_{oc}(T_c) = \frac{nkT}{q} ln\left(1 + \frac{J_{sc}}{J_o(T_c)}\right) \quad (2.7)$$

If the value of Jsc is very large compared to J_o, equation (7) can be written:

$$V_{oc}(T_c) = \frac{nkT}{q} lnJ_{sc} - \frac{nkT}{q} lnJ_o(T_c) \quad (2.8)$$

This open circuit voltage depends on the meteorological conditions of the study area, ie temperature and irradiance:

$$V_{oc}(T_c, C) = \frac{nkT_c}{q} ln\left(\frac{C \times J_{sc}}{J_o(T_c)}\right) \quad (2.9)$$

where n is the ideality factor, k is the Boltzmann constant, C is the incident power ratio, and J_o is the inverse saturation current density which represents a recombination phenomenon in the neutral regions and is given by [22]:

$$J_o(T_c) = q\left(\frac{D_e}{L_n N_A} + \frac{D_h}{L_p N_D}\right) {n_i}^2(T_c) \quad (2.10)$$

where n_i is the intrinsic concentration, D_e and D_h are the diffusion coefficients of the electrons and holes respectively, L_n and L_p are the diffusion lengths of the minority carriers in the $n - type$ and $p - type$ materials, N_A and N_D are the concentrations of impurity acceptors and donors. For the typical levels of donor and acceptor impurity concentration for which $N_A \simeq 10^{17} cm^{-3}$ and $N_D \simeq 10^{18} cm^{-3}$, the parenthetical term in equation (10) can be neglected, so we have [22] :

$$J_o(T_c) = q{n_i}^2(T_c) \quad (2.11)$$

with

$$\begin{aligned} {n_i}^2 &= N_c N_v exp(\frac{-E_g}{kT_c}) \\ &= 4\left(\frac{2\pi kT_c}{h^2}\right)^3 {m_e}^{*\frac{3}{2}} {m_h}^{*\frac{3}{2}} exp\left(\frac{-E_g}{kT_c}\right) \end{aligned} \quad (2.12)$$

where Nc and Nv are effective densities of electrons and holes, $h$is the Planck constant, ${m_e}^*$ and ${m_h}^*$ are effective masses of electrons and holes, E_g is the gap energy of the semiconductor used. If we replace equation (12) in (11), we have:

$$J_o(T_c) = 4q\left(\frac{2\pi kT_c}{h^2}\right)^3 {m_e}^{*\frac{3}{2}} {m_h}^{*\frac{3}{2}} exp\left(\frac{-E_g}{kT_c}\right) \quad (2.13)$$

To determine the maximum power point (P_{max}), the current-voltage characteristic of a single junction solar cell must be taken into account:

$$J = J_{sc} + J_o\left(exp\left(\frac{qV}{kT}\right) - 1\right) \quad (2.14)$$

The maximum power P depending on the voltage must be found as follows:

$$P = VJ = V\left[J_{sc} + J_o\left(exp\left(\frac{qV}{kT}\right) - 1\right)\right] \quad (2.15)$$

the point of maximum power can be calculated by defining the derivative equal to zero [23]:

$$\left(\frac{dP}{dV}\right)_{V_m} = -J_{sc} - J_o + J_o\left(1 + \frac{qV_m}{kT}\right) exp\left(\frac{qV_m}{kT}\right) = 0 \quad (2.16)$$

To calculate the efficiency as a function of the concentration, it is necessary to find the power at the maximum point which is given according to J_{sc}, J_o and T(Eqs 15 and 16).The equation (16) for the maximum voltage cannot be solved explicitly, but by posing that:

$$ln\left(1 + \frac{qV_m}{kT}\right) \approx a \quad (2.17)$$

a is a constant.

For many sub-cells used, the voltage at the maximum point is between $0.5V$ and $2V$; this corresponds to the value of the constant between 3.02 and 4.37. Which gives a good average of the value of $a = 3.69$. The maximum voltage (V_{max}) is obtained according to the relation [24]:

$$V_{max} = \frac{nkT_c}{q}\left[ln\left(\frac{C \times J_{sc}}{J_o(T_c)}\right) - a\right] \quad (2.18)$$

The maximum power will be given by the relations (19) and (20) [25]:

$$P_{max} = J_{sc}\,(exp(-a) - 1) \times V_{max} \quad (2.19)$$

$$P_{max} = J_{sc}\,(exp(-a) - 1) \times \frac{nkT_c}{q}\left[ln\left(\frac{C \times J_{sc}}{J_o(T_c)}\right) - a\right] \quad (2.20)$$

For the calculation of fill factor (FF) and the conversion efficiency (η), we use the following analytic formula [26]:

$$FF = \frac{Voc - nV_t ln\left(\frac{Voc}{nVt+0.72}\right)}{Voc + nV_t} \quad (2.21)$$

Where $V_t = \frac{kT}{q}$ is the thermal tension.

The conversion efficiency will be calculated using the expression (22):

$$\eta = \frac{FF \times Voc \times Jsc}{P_{in}} \quad (2.22)$$

where P_{in} is the incident power.

3 RESULTS AND DISCUSSION

This work consists of developing an analytical model to analyze the behavior of the sub-cell output parameters of the $Ga_{0.67}In_{0.33}P/GaAs/Ga_{0.70}In_{0.30}As$ tri-junction photovoltaic cell and finally to predict the maximum electrical power produced by this cell in the actual weather conditions of the selected sites. We choose for our case two sites namely Bujumbura and Bugarama.The Bujumbura site is located in the relatively hot region of Imbo and the Bugarama site is located in the mountainous area where the average monthly temperature is low compared to that of Bujumbura.The first thing to do is to determine what is the daily variation in irradiance and temperature in these sites. We used the data available in the MERRA (Modern-Era Retrospective Analysis for Research and Applications) databases.In practice, it is mainly the data of the worst month (rainy season in the tropical and equatorial zone) which interest us because the objective is to know if our photovoltaic cell is able to cover the energy needs of all the year once installed at this location. The best month data (dry season in the tropical and equatorial zone) can also be interesting to get an idea of the maximum production of the cell. To make our data more reliable, we calculated the data for a typical day (TD) for the lightest month and the sunniest month.These data are found by averaging the temperature and irradiance of each hour, each day of April and September.

By analyzing the data for the two selected sites, we find that the average daily temperature (typical day of September and April) for the Bujumbura site is higher than that of the Bugarama site. On the other hand, we notice that the average daily irradiance (typical day of September) for the Bujumbura site is lower than that of the Bugarama site, which is not the case for the typical day of April (Figure 2).

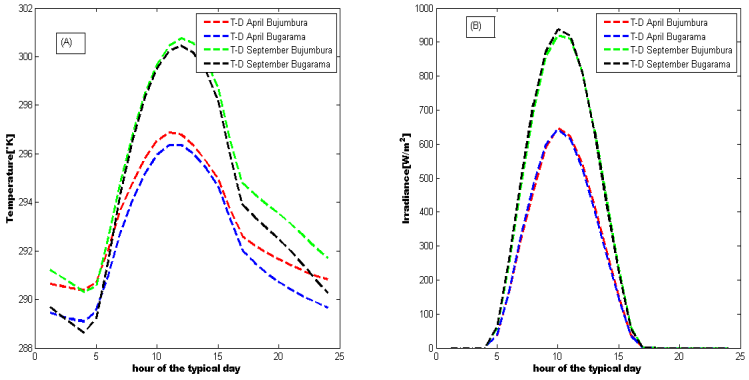

Fig. 2. Daily variation (A) of the temperature and (B) of the irradiance for the typical days(TD) of the months September and April 2018 of the sites of Bujumbura and Bugarama (Burundi).

Figures (2 and 3) show the daily variation of the external quantum efficiency (EQE) of the three sub-cells of the $Ga_{0.67}In_{0.33}P/GaAs/Ga_{0.70}In_{0.30}As$ tri-junction photovoltaic cell for the typical day of the months September and April of the sites of Bujumbura and Bugarama.These EQE are plotted as a function of the wavelengths corresponding to the absorption ranges of the sub-cells.

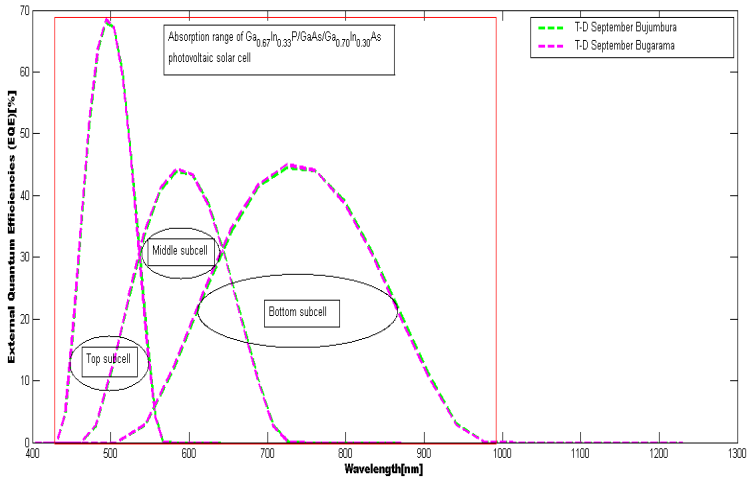

Fig. 3. Daily variation of the External Quantum Efficiency (EQE) of the three sub-cells of the $Ga_{0.67}In_{0.33}P/GaAs/Ga_{0.70}In_{0.30}As$ tri-junction photovoltaic cell for the typical day of September on the sites of Bujumbura and Bugarama (Burundi).

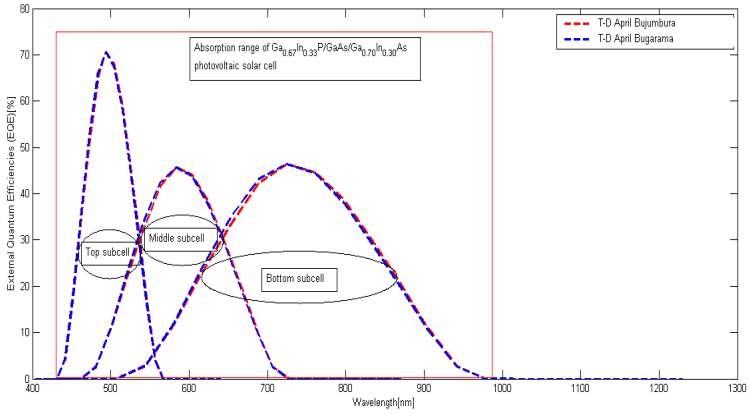

Fig. 4. Daily variation of the External Quantum Efficiency (EQE) of the three sub-cells of the $Ga_{0.67}In_{0.33}P/GaAs/Ga_{0.70}In_{0.30}As$ tri-junction photovoltaic cell for the typical day of April on the sites of Bujumbura and Bugarama (Burundi).

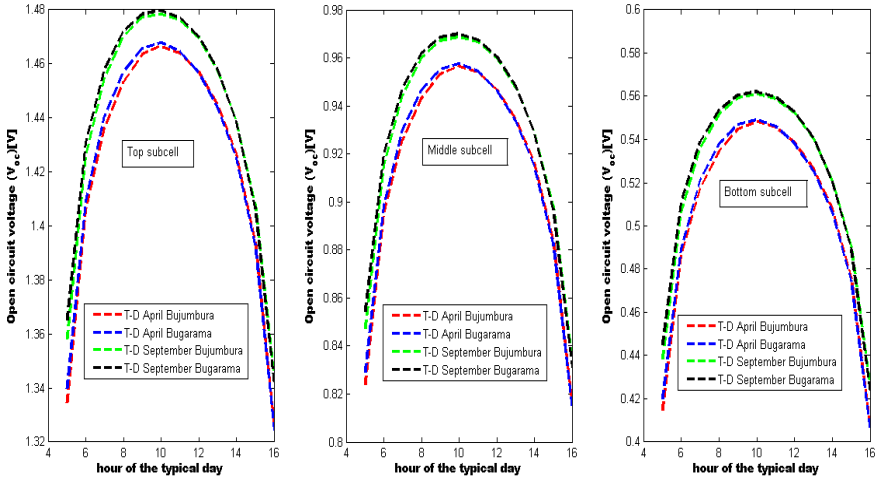

Fig. 5. Daily variation of the open circuit voltage (V_{oc}) of the three sub-cells of the $Ga_{0.67}In_{0.33}P/GaAs/Ga_{0.70}In_{0.30}As$ tri-junction photovoltaic cell for the typical day of April and September on the sites of Bujumbura and Bugarama (Burundi).

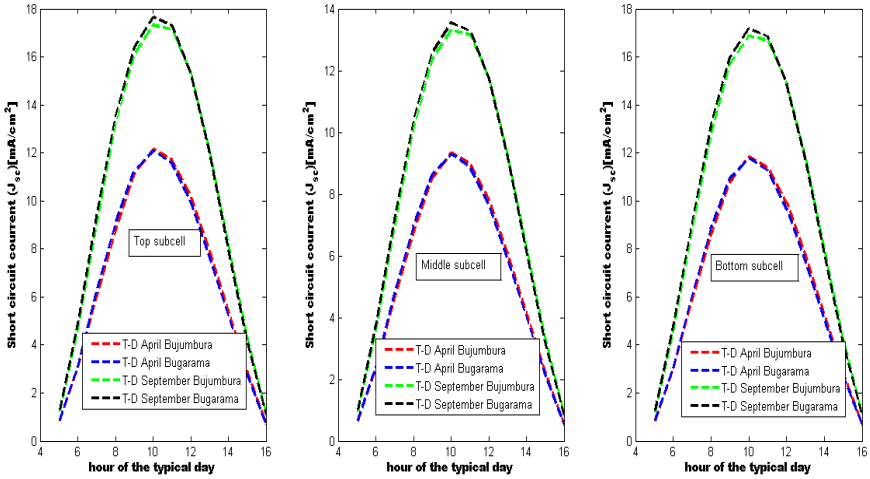

Fig. 6. Daily variation of the short-circuit current density (J_{sc}) of the three sub-cells of the $Ga_{0.67}In_{0.33}P/GaAs/Ga_{0.70}In_{0.30}As$ tri-junction photovoltaic cell for the typical day of April and September on the sites of Bujumbura and Bugarama (Burundi).

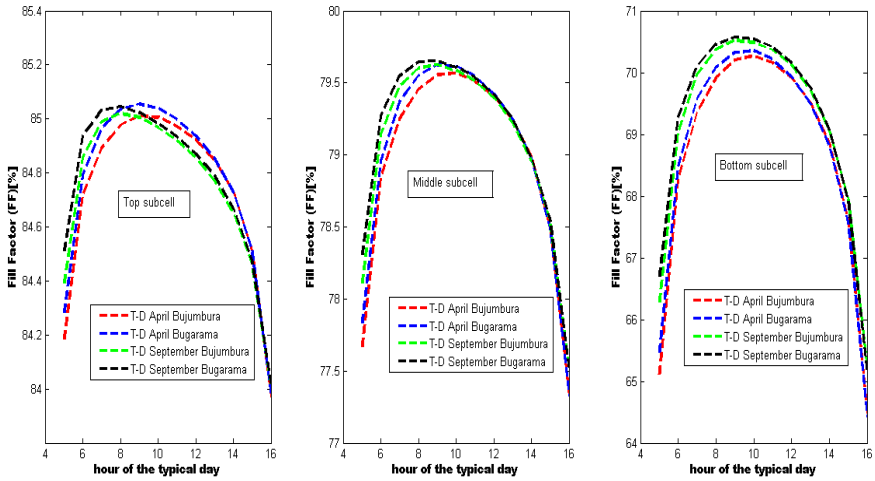

Fig. 7. Daily variation of the Fill Factor (FF) of the three sub-cells of the $Ga_{0.67}In_{0.33}P/GaAs/Ga_{0.70}In_{0.30}As$ tri-junction photovoltaic cell for the typical day of April and September on the sites of Bujumbura and Bugarama (Burundi).

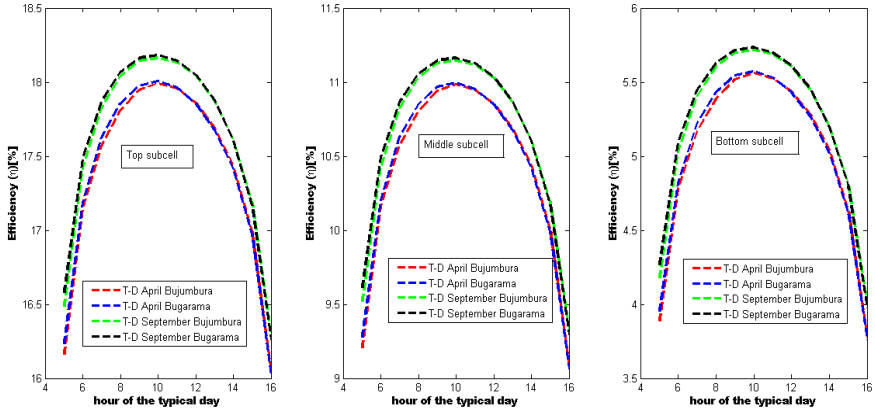

Fig. 8. Daily variation of the conversion efficiency (η) of the three sub-cells of the $Ga_{0.67}In_{0.33}P/GaAs/Ga_{0.70}In_{0.30}As$ tri-junction photovoltaic cell for the typical day of April and September on the sites of Bujumbura and Bugarama (Burundi).

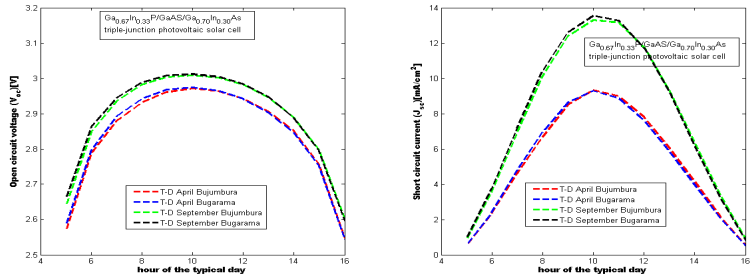

Fig. 9. Daily variation of the open circuit voltage (V_{oc}) and the short circuit current density (Jsc) of the $Ga_{0.67}In_{0.33}P/GaAs/Ga_{0.70}In_{0.30}As$ tri-junction photovoltaic cell for the typical day of April and September on the sites of Bujumbura and Bugarama (Burundi).

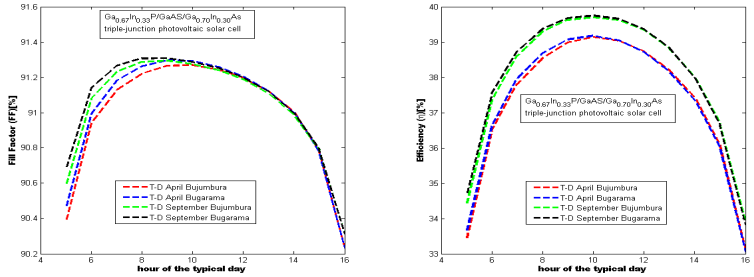

Fig. 10. Daily variation of the form factor (FF) and the conversion efficiency (η) of the $Ga_{0.67}In_{0.33}P/GaAs/Ga_{0.70}In_{0.30}As$tri-junction photovoltaic solar cell for the typical day of April and September on the sites of Bujumbura and Bugarama (Burundi).

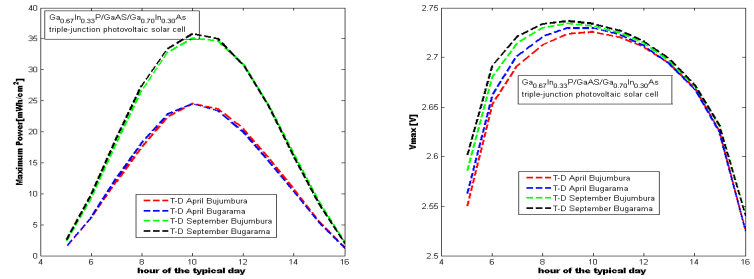

Fig. 11. Daily variation of the maximum power (P_{max}) and the maximum voltage (V_{max}) of the $Ga_{0.67}In_{0.33}P/GaAs/Ga_{0.70}In_{0.30}As$ tri-junction photovoltaic cell for the typical day of April and September on the sites of Bujumbura and Bugarama (Burundi).

Table 4. The output parameters of the $Ga_{0.67}In_{0.33}P/GaAs/Ga_{0.70}In_{0.30}As$ tri-junction photovoltaic cell for the typical day of April and September on sites of Bujumbura and Bugarama (Burundi).

Parameters	JT Avr Bujumbura	JT Avril Bugarama	JT Sept Bujumbura	JT Sept Bugarama
Voc [V]	34.06	34.10	34.63	34.68
Jsc [mA/cm^2]	61.76	61.53	91.79	92.05
FF [%]	90.98	91.00	91.03	91.05
η [%]	37.24	37.28	37.94	38.00
P$_{max}[W/m^2]$	1613.1	1619.7	2405.1	2431

The EQE is considered as a quantitative and qualitative parameter in the description of a solar cell. It allows the quantification of losses in the solar cell (reflection on the surface, losses of low and high energy photons). Quantum efficiency is a size that lets you know in which wavelength range the solar cell responds best. We can thus deduce information related to the quality of materials and contacts. We find that the $Ga_{0.67}In_{0.33}P/GaAs/Ga_{0.70}In_{0.30}As$ tri-junction photovoltaic cell responds better in the range from $430nm$ to $980nm$. The top sub-cell $(Ga_{0.67}In_{0.33}P)$ is effective in the range from $430nm$ to $570nm$, with its peak at $490nm$, that of the middle $(GaAs)$ in the range from $500nm$ to $700nm$, with its peak at $600nm$ and the bottom cell $(Ga_{0.70}In_{0.30}As)$ in the range from $600nm$ to $980nm$, with its peak at $700nm$. These results are almost valid for all sites considered and for all typical days of selected months.The percentages of the peaks of the sub-cells are higher for the typical day which has a higher irradiance. The maximum EQE of all the sub-cells is reached at $10:00AM$ for all the typical days of all the months considered and on all the chosen sites.

We find that the EQE follows the daily variation of the irradiance and reaches its maximum when the irradiance becomes maximal during the day. In addition, we notice a discreet shift of the EQE of each sub-cell towards long wavelengths for the months of September and April on the site of Bujumbura. This is due to a high daily temperature for these months at the Bujumbura site compared to that of the Bugarama site. This shift is directly related to the shift of the absorption range of the sub-cells due to the dependence of their band gap at the temperature.

Figures (5), (6), (7) and (8) show the daily variations of the open circuit voltage (V_{oc}), the short circuit current density (J_{sc}), the fill factor (FF) and the efficiency (η) of the Top $(Ga_{0.67}In_{0.33}P)$, Middle $(GaAs)$ and Bottom $(Ga_{0.70}In_{0.30}As)$ sub-cells for the typical days of the months of September and April 2018 at the two selected sites. We find that the daily open circuit voltage (V_{oc}) of all the sub-cells (top, middle and bottom) is higher for the typical day of September at the Bugarama site which has received a higher overall daily radiation (Figure 2B). The same behavior manifests itself for all the typical days of the months and sites considered. We notice that the open circuit voltage increases logarithmically with the incident power in accordance with equation (2.9). It is the same for the daily short-circuit current density (J_{sc}), it is maximum for the typical day of September on the site of Bugarama. The same behavior manifests itself for all the typical days of the months and sites considered. The short circuit current density increases linearly with irradiance in accordance with equation (2.6). What justifies this slope of the curves of the daily variation of the short-circuit current density (J_{sc}) of the figure (6).

The fill factor (FF) is a function of the open circuit voltage and the thermal voltage according to equation (2.21). It increases when the temperature decreases in agreement with our results which show a maximum fill factor for all the sub-cells for the typical days of April and September at the Bugarama site (Figure 7 and Table 1), where the average daily temperature is the lowest, compared to the results found for the typical days of April and September at the site of Bujumbura, where the average daily temperature is higher than that of Bugarama.

The conversion efficiency (η) is mainly a function of the open circuit voltage and the short-circuit current density and the incident power. As the short circuit current density (J_{sc}) increases linearly with the incident power, it does not affect the efficiency. The open circuit voltage increases logarithmically with the incident power and necessarily affects the efficiency. The conversion efficiency of all sub-cells is maximum for the month of September at the Bugarama site (Figure 8) where the global daily radiation is greater (Figure 8 and Table 1). This is due to the high value of the open circuit voltage there at this time due to high incident power (Figure 5).

All the results found concerning the behavior of the open circuit voltage (V_{oc}) , the short circuit current density (J_{sc}), the fill factor (FF) and the conversion efficiency (η) for the sub-cells are also valid on the $Ga_{0.67}In_{0.33}P/GaAs/Ga_{0.70}In_{0.30}As$ Tri-Junction solar cell as shown in figures (9-10).

Figure (11) shows the daily variation of the voltage at the maximum point (V_{max}) and the power (P_{max}) of the $Ga_{0.67}In_{0.33}P/GaAs/Ga_{0.70}In_{0.30}As$ tri-junction photovoltaic cell for the typical day of April and September in Bujumbura and Bugarama (Burundi) sites.

We found that (V_{max}) is maximum where the incident power is higher as is the case for the (V_{oc}). This is the same observation for the power produced by the cell. If the results found in this work should be taken into consideration when sizing the installation of a photovoltaic system composed of $Ga_{0.67}In_{0.33}P/GaAs/Ga_{0.70}In_{0.30}As$ tri-junction photovoltaic solar cell; the results found for the worst month (April) should be used for the Bujumbura and Bugarama sites. An average daily conversion efficiency of 37.24% for the typical day of April and a daily power of $1613.1W/m^2$ were found on the site of Bujumbura and an average daily efficiency of 37.28% and a power of $1619.7W/m^2$ for the Bugarama site. The September results at the Bujumbura and Bugarama sites can be used to calculate the maximum average conversion efficiency and the maximum power produced by the Tri-junction solar cell.

4 CONCLUSION

In this work, we studied the behavior of the output parameters of the sub-cells composing the $Ga_{0.67}In_{0.33}P/GaAs/Ga_{0.70}In_{0.30}As$ tri-junction photovoltaic solar cell and the daily energy production of this cell operating under the actual weather conditions of selected sites in Burundi.For our study, two sites were chosen, namely Bujumbura, which is located in the hottest part of the country, and the Bugarama site in the mountainous zone, where the average daily temperature is low compared to that of Bujumbura. We were interested in the two reference months, the month of September which is the sunniest for the two sites and the month of April which is the least sunny.

An analytical model to analyze the behavior of the output parameters of the sub-cells composing the $Ga_{0.67}In_{0.33}P/GaAs/Ga_{0.70}In_{0.30}As$ tri-junction photovoltaic solar cell and finally to predict the maximum electrical power produced by this cell taking into account the actual weather conditions (Irradiance and temperature) of the selected sites has been developed. An External Quantum Efficiency EQE of all sub-cells, which is a quantitative and qualitative parameter in the description of a solar cell, was calculated for the typical days of September and April for all the two sites considered.This EQE follows the daily variation of the irradiance and reaches its maximum when the irradiance becomes maximal during the day.In addition, we noticed a discreet shift of the EQE of each sub-cell towards long wavelengths for the months of September and April at the Bujumbura site. This is due to a high daily temperature for these months at the Bujumbura site compared to that of the Bugarama site. The meteorological factors to which we attached importance in this study (irradiance and temperature) strongly influence the output parameters of the sub-cells studied. We found an average daily open circuit voltage (V_{oc}) of all sub-cells (top, middle and bottom) which is higher for the typical day of the sunniest month. It is the same for the daily average of the short-circuit current density (J_{sc}), both are maximum for the month of September on the Bugarama site.The fill factor (FF) increases with decreasing temperature in accordance with our results. They show a maximum fill factor

for all sub-cells in September and April at the Bugarama site where the average daily temperature is the lowest.On the other hand, conversion efficiency is highest for all sub-cells in September at the Bugarama site, where the average daily global radiation is higher.In addition, the daily power produced (P_{max}) by $Ga_{0.67}In_{0.33}P/GaAs/Ga_{0.70}In_{0.30}As$ tri-junction photovoltaic solar cell is maximum for the typical day of September at the Bugarama site where the incident power is high.

ACKNOWLEDGEMENT

The authors are grateful to the reviewers for their careful reading, constructive criticisms, comments and suggestions, which have helped us to improve this work significantly.

COMPETING INTERESTS

Authors have declared that no competing interests exist.

REFERENCES

[1] Houée P. Opportunités dans le secteur des energies renouvelables au Burundi. Bujumbura; 2016.

[2] Nsengiyumva A., Impact d'électrification des zones rurales, par des systèmes photovoltaïque autonomes, sur léconomie Burundaise. Revue Des En. Ren. 2017;20:471-482.

[3] Nelson CA, et al. Exceeding the Shockley-Queisser limit in solar energy conversion. Energy Environ.Sci. 2013;6:3508.

[4] Vanessa G. Caractrisations de matriaux et tests de composants des cellules solaires a' base des nitrures des lments III-V. The'se, Universit Paris-Sud. 2012;11.

[5] Fan JCC. Theoretical temperature dependence of solar cell parameters, Solar Cells. 1986;17(23):309315.
DOI.10.1016/0379- 6787(86)90020-7.

[6] Siefer G, Bett AW. Analysis of temperature coefficients for IIIV multi-junction concentrator cells. Progress in Photovoltaic: Research and Applications. 2012;10.1002/pip.2285.

[7] Aiken D, Stan M, Murray C, Sharps P, Hills J, Clevenger B. Temperature dependent spectral response measurements for IIIV multi-junction solar cells. In Proceedings of the 29th IEEE Photovoltaic Specialists Conference, New Orleans,USA. 2002;828831.
DOI: 10.1109/PVSC.2002.1190704.

[8] Steiner MA, Geisz JF, Friedman DJ, Olavarria WJ, Duda A, Moriarty T. Temperature-dependent measurements of an inverted metamorphic multi-junction (IMM) solar cell. In Proceedings of the 37th IEEE Photovoltaic Specialists Conference,Seattle,USA. 2011;25272532.
DOI:10.1109/PVSC.2011.6186461.

[9] Peharz G, Rodriguez JPF, Siefer G, Bett AW. A method for using CPV modules as temperature sensors and its application to rating procedures. Solar Energy Materials and Solar Cells. 2011;95(10):27342744.

[10] Ahmed M. Yahya, Youm I, Kader A. Behavior and performance of a photovoltaic generator in real time. IJPS. 2011;6(18):4361-4367.

[11] Nzigidahera B. et Sinarinzi, Etude de Vulnérabilité et d'adaptation aux changements climatiques au Burundi. Bujumbura; 2006.

[12] Haas J. Wilcox, Gray J, Schwartz R. Design of A GaInP/GaAs tandem solar cell for maximum daily, monthly, an yearly energy out- put. Journal of Photonics for Energy. 2011;1.

[13] Sze SM. Physics of semiconductors devices. Second Edition, John Wiley and Sons; 2001.

[14] Evoy A. Mc, Markvart T, Castener L. Practical handbook of photovoltaics fundamental and application. Second Edition Elsevier Ltd; 2012.
ISBN:978-0-12-3859334-1.

[15] Adachi S. $GaAs$,$AlAs$ and $Al_xGa_{1x}As$: Material parameters for use in research and Devise application. J. Appl. Phys. 1985;58(3):R1-R29.

[16] Goldberg YA. Handbook Series on semiconductor parameters. World Scientific, London. 1999;2.

[17] Ryan A. Modeling solutions and simulations for advanced III-V photovoltaic based on nanostructures. Master of science thesis Rochester Institute of technology Rochester, NY; 2008.

[18] Martin A. Green. Solar cells: Operating principles, technology, and system application. Prentice-Hall Series in Solid State Physical Electronics; 1982.
ISBN-13: 978-0138222703.

[19] De Soto W, Klein SA, Beckman WA. Improvement and validation of a model for photovoltaic array performance. Solar Energy Laboratory, University of Wisconsin-Madison, 1500 Engineering Drive, Madison, WI 53706, USA; 2005.

[20] Ayaz R, Nakir I, Tanrioven M. An improved matlab-simulink model of PV module considering ambient conditions. International Journal of Photoenergy; 2014.

[21] Hegedus S, Shafarman WN. Thin-Film solar cells: Devise analysis and measurements. Progress in Photovoltaic: Research and Application. 2004;12:155-176.

[22] Hu C, White RM. Solar cells. New York: McGraw-Hill. 1983;21.

[23] Gerald Siefer, Andreas W. Bett. Analysis of temperature coefficients for IIIV multijunction concentrator cells. Fraunhofer Institute for Solar Energy Systems ISE; 2012.

[24] Matthias E. Nell. The spectral p-n junction model for tandem solar-cell design. IEEE Transaction on Electron Devices. 1987;ED-34(2).

[25] Nell ME, Barnett AM. A $GaAs_{1-x}P_x$ top tandem solar cell with high performance, in Proc. 6th E. C. European Photovoltaic Solar Energy Conf. 1985;265-269.

[26] Writing G. Global energy assessment, toward a sustainable future. First Edition, Cambridge University Press; 2012.
ISBN: 978052118.

Peer-review history:
The peer review history for this paper can be accessed here:
http://www.sdiarticle4.com/review-history/51593